

DETERMINATION OF ANISOTROPY CONSTANTS FOR MONOCLINIC FERROMAGNETIC COMPOUNDS

S. WIRTH, M. WOLF, A. MARGARIAN* and K.-H. MÜLLER

Institut für Festkörper- und Werkstofforschung Dresden,

D-01171 Dresden, P.O. Box 20 00 27, Germany

**CSIRO Division of Applied Physics, Lindfield NSW 2070, Australia*

ABSTRACT

There is much interest in the intrinsic magnetic properties of R_3T_{29} compounds (R - rare earth, T - transition metal) or the interstitially modified phases $R_3T_{29}N_x$. These phases reveal a monoclinic crystalline structure. Therefore, contrary to the case of uniaxial (i.e. tetragonal, hexagonal or rhombohedral) materials, two anisotropy constants are necessary to describe the magnetocrystalline anisotropy energy already in lowest order in a series expansion of direction cosines. Furthermore, the discussion of the origin of the magnetic anisotropy in R-T compounds showed, that both these constants have to be expected to have the same order of magnitude. Thus, the well established methods to determine the second and fourth order anisotropy constants K_1 and K_2 for uniaxial compounds from demagnetization curves had to be completely revised for the 3:29 compounds. We developed a fit-procedure which enables the determination of the two anisotropy constants (of lowest order) in monoclinic phases from the demagnetization curves of polycrystalline samples, measured in the range of reversible rotational processes. The procedure has been applied to $R_3(Fe,Ti)_{29}$ with R = Sm, Nd, Pr and Ce and to the interstitially modified nitrides $R_3T_{29}N_x$ ($x = 4$) with R = Sm, Nd and Pr.

1. Introduction

The structural and magnetic properties of compounds $R_3(Fe,M)_{29}$ ¹⁻⁴ (where R is a 4f-element and M is a metal such as Ti or V added in small amounts to stabilize the 3:29 structure) are of interest not only because of their hard magnetic properties but also from a physical point of view: (i) the monoclinic 3:29 structure like its rhombohedral 2:17 and tetragonal 1:12 counterparts can be derived from the same 1:5 parent structure by replacing a part of the R atoms by Fe dumb-bells^{1,3} and (ii) these as well as the corresponding interstitially modified compounds consist of two types of segments. In one of them the R ions have nearly the same environment as in the rhombohedral R_2Fe_{17} structure, whereas in the other ones the environment is the same as in the tetragonal $R(Fe,M)_{12}$.^{1,3,4} Using well established methods for the investigation of uniaxial (i.e. tetragonal, hexagonal or rhombohedral) materials controversial results for the magnetocrystalline anisotropy have been reported.^{4,5} It should be noted, however, that the

magnetic anisotropy of monoclinic crystals cannot be described by the anisotropy constants K_1, K_2, \dots used for uniaxial systems.

In this investigation the magnetic anisotropy of monoclinic materials will be described in lowest order of the expansion series in direction cosines. Demagnetization curves in the range of reversible rotational magnetization processes will be calculated for polycrystalline samples and then fitted to curves measured for $R_3(Fe,M)_{29}$ compounds, with $R = Sm, Nd, Pr$ and Ce and some of their nitrides. A superposition model of the magnetic anisotropy of the nitrides will be developed taking into account structural relations of the 1:12 and the 2:17 segments to the 3:29 structure and the effect of crystalline electric fields (CEF) of the interstitial N atoms.

2. Experimental

Single phase $R_3(Fe,Ti)_{29}$ (≈ 6.3 at.% Ti) compounds with $R = Sm, Nd, Pr$ and Ce were prepared by melting in an induction furnace and by homogenizing at $1050^\circ C$ for 40 hours. Microstructural characterization was made by X-ray diffraction and scanning electron microscopy. The material was crushed and then milled in a vibrating ball mill for 100 min. For nitrogenation the milled powders were annealed in N_2 at $360-480^\circ C$ for 3–20 hours. The content of N was determined by the mass gain and by the heat extraction method. Textured samples were obtained by compacting the powders in aligning fields of 2 T. Magnetic measurements have been conducted in a VSM with fields up to 8 T.

3. Description of Magnetic Anisotropy in the Monoclinic 3:29 Phase

3.1. Structure of the 3:29 Phase

The relations between the 1:5, 1:12, 2:17 and 3:29 R-Fe structures can be summarized as follows:¹⁻⁴ Substituting a certain fraction δ of the R atoms by Fe dumbbells in the parent structure of $CaCu_5$ -type results in (i) the 1:12 structure ($\delta = 1/2$) being tetragonal with space group $I4/mmm$, (ii) the 2:17 structure ($\delta = 1/3$) being rhombohedral with space group $R\bar{3}m$ in the case of light R and (iii) the monoclinic 3:29 phase ($\delta = 2/5$) which is not only formally related to the 1:12 and 2:17 structures by



but consists of appropriately stacked 1:12 and 2:17 segments. The point group controlling magnetic anisotropy is $2/m$ for both the two space groups $P2_1/c$ and $A2/m$ under discussion for the 3:29 phase.²⁻⁴ Additionally to the monoclinic a_m, c_m and the two-fold b_m axes, two axes c_r and c_t are defined to be the c-axes of the rhombohedral 2:17 and tetragonal 1:12 segments, respectively. The axes b_m, c_r , and c_t are perpendicular to each other. Introducing nitrogen into these compounds leads to small lattice expansions result-

ing in an enhancement of the Curie temperature and in the case of $\text{Sm}_3(\text{Fe},\text{M})_{29}$ to a reorientation of easy magnetization direction (EMD). The structure type formed by the R and Fe atoms remains unchanged. The local environment of the R atoms in $\text{R}_3(\text{Fe},\text{M})_{29}\text{N}_4$ with regard to the interstitial N atoms is the same as expected according to Eq.1, i.e. 2 R atoms with a 1:12 environment and 4 R atoms with a 2:17 one per unit cell. These structural features are shown in Fig.1.

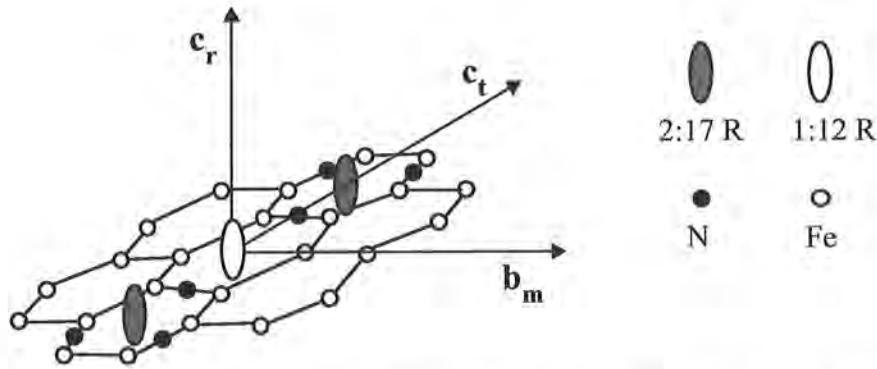


Fig.1 : R atoms in the 3:29 structure and the two types of their environment (1:12 and 2:17). b_m is the two-fold monoclinic axis, c_r and c_t are the c axes of the 2:17 and 1:12 segments, respectively, forming the 3:29 phase.

3.2. Magnetic Anisotropy

It is well known that the magnetocrystalline energy density f_A can formally be expressed as an expansion series in the direction cosines with respect to an arbitrary Cartesian coordinate system.^{6,7} For tetragonal and rhombohedral systems the lowest (i.e. second) order of this expansion is reduced to one term

$$f_{At} = K_{1,t} \sin^2 \vartheta_t \quad (2a)$$

$$f_{Ar} = K_{1,r} \sin^2 \vartheta_r \quad (2b)$$

where ϑ_t and ϑ_r are the polar angles of the local spontaneous magnetization \mathbf{J}_s with respect to the axes c_t and c_r , respectively. $K_{1,t}$ and $K_{1,r}$ are the corresponding "first" anisotropy constants. In the case of monoclinic crystals the generalization of Eqs.2a and 2b is

$$f_{Am} = K_{1\vartheta} \sin^2 \vartheta + K_{1\varphi} \sin^2 \vartheta (1 + \cos 2\varphi) \quad (3)$$

where ϑ is the polar angle of \mathbf{J}_s with respect to an axis arbitrarily chosen out of the three principal axes of the energy density f_{Am} , and φ is the azimuth angle relative to one of the two other principal axes. It should be noted that (i) the two-fold monoclinic b_m axis is one of the principal axes and (ii) the system has always an EMD which is one of the principal axes (but not necessarily the b_m axis). Magnetic anisotropy of types easy plane or easy cone are impossible in monoclinic systems even in lowest, i.e. second, order in the direction cosines. In this investigation, the angle ϑ in Eq.3 is referred to the EMD and φ to the magnetically hard direction. Therefore, both $K_{1\vartheta}$ and $K_{1\varphi}$ are non-negative.

In the considered R-Fe compounds the 4f-charge cloud is strongly exchange coupled to the 3d-electrons of Fe which give rise to the magnetization. Hence, a change of the direction of the magnetization \mathbf{J}_s implies a rotation of the 4f-charge cloud. Thereby the CEF anisotropy is transferred into the magnetic system. For $R_2Fe_{17}N_3$ and $R(Fe,M)_{12}N$ the anisotropy is dominated by the CEF effects of the N atoms, where only nearest N-neighbours of the R atoms contribute to the anisotropy significantly. Taking into account this mechanism and the structure relations between the 3:29 (m), 1:12 (t) and 2:17 (r) structures, f_{Am} should be given by the weighted sum of the anisotropy energy densities f_{At} and f_{Ar} (superposition principle). Calculating f_{Am} one has to take into account that ϑ_t and ϑ_r refer to different axes. To be more specific $Sm_3Fe_{29}N_4$ is considered in the following. We relate the polar and azimuth angles to the 2:17 axes, $(\vartheta, \varphi) \equiv (\vartheta_r, \varphi_r)$, and rewrite f_{At} :

$$f_{At} = -K_{1,t}/2 \sin^2 \vartheta_r - K_{1,t}/2 \sin^2 \vartheta_r \cos 2\varphi_r \quad (4)$$

Then f_{Am} is given by

$$f_{Am} = \left(\frac{2v_r}{3v_m} K_{1,r} - \frac{v_t}{2v_m} K_{1,t} \right) \sin^2 \vartheta_r - \frac{v_t}{2v_m} K_{1,t} \sin^2 \vartheta_r \cos 2\varphi_r \quad (5)$$

which, as expected, has the form of Eq.3. The factors $2v_r/3v_m$ and $v_t/2v_m$ (v_r, v_m, v_t - volume of the unit cells) take into account that the energy contributions of the different R^{3+} ions in the 3:29 phase have to be summed up. In $Sm(Fe,M)_{12}N$ and $Sm_2Fe_{17}N_3$ we have $K_{1,t} < 0$ and $K_{1,r} > 0$, respectively.⁸⁻¹¹ Thus, in the case of $Sm_3(Fe,M)_{29}N_4$, $K_{1,r}$ and $K_{1,t}$ have a similar influence on the contribution not depending on φ in Eqs.3 and 5 and the axis c_r turns out to be the EMD which is in agreement with results of X-ray investigations.⁵ The two other principal axes are b_m and c_t . These results can be understood by looking at the interaction between the N atoms and the 4f-clouds when rotating the magnetization direction (cf. Fig.1): The direction of axis of rotation of the

prolate 4f-charge cloud is parallel to \mathbf{J}_s . A rotation of \mathbf{J}_s implies a rotation of the 4f-charge cloud into the same direction. Moving \mathbf{J}_s from the EMD to the c_t - b_m -plane increases the energy of electrostatic interaction between the 4f-charges and the N atoms and thus f_{Am} . This increase becomes maximum at $(\vartheta_r = \pi/2, \varphi_r = 0)$, i.e. if \mathbf{J}_s is parallel to the c_t -axis since in that case the energy of the Sm^{3+} ions in the 2:17 as well as that in the 1:12 environment is increased. Thus c_t is the magnetically hard direction. \mathbf{J}_s parallel to the b_m -axis $(\vartheta_r = \pi/2, \varphi_r = \pi/2)$ results in an intermediate value of f_{Am} as the energy of the 2:17 type Sm^{3+} ions is increased whereas that of the 1:12 type ions remains unchanged.

4. Experimental determination of magnetocrystalline anisotropy

4.1. Reversible magnetization processes in materials of monoclinic structure

The anisotropy constants of a uniaxial material can be determined by fitting demagnetization curves of polycrystalline samples, calculated in the range of reversible rotational magnetization processes, to measured curves.⁸

In-plane anisotropies in uniaxial materials are at least of the fourth order and of fourfold symmetry. Therefore, the reversible rotation of the grain polarizations can be well considered to take place in a plane given by the grain EMD and the field direction only. This rotational behaviour of the polarization is completely changed in case of the 3:29 compound as easily can be seen from Eq.3 where $K_{1\vartheta}$ and $K_{1\varphi}$ are of the same order of magnitude. Now, the equilibrium orientation of the saturation polarization \mathbf{J}_s has to be determined from the minimum of the energy density

$$f_m = K_{1\vartheta} \sin^2 \vartheta + K_{1\varphi} \sin^2 \vartheta (1 + \cos 2\varphi) - H J_s \cos \eta \Rightarrow \text{Min.} \quad (6)$$

Here, η denotes the angle between \mathbf{J}_s and \mathbf{H} . The orientation of \mathbf{J}_s calculated from Eq.6 for different directions and magnitudes of \mathbf{H} is illustrated in Fig.2 where the values $K_{1\vartheta} = 4 \text{ MJm}^{-3}$, $K_{1\varphi} = 5.2 \text{ MJm}^{-3}$ and $J_s = 1.3 \text{ T}$ have been used which are expected to be in the order of magnitude as those of $\text{Sm}_3(\text{Fe},\text{M})_{29}\text{N}_4$. As discussed in Section 3.2 c_r is the EMD of $\text{Sm}_3(\text{Fe},\text{M})_{29}\text{N}_4$, b_m is the direction of intermediate anisotropy and c_t is the hard direction. The directions of \mathbf{H} used for the calculated curves of Fig.2 (shown by circled markers) are (i) polar angle $\Theta_r = 90^\circ$ and azimuth angles $\Phi_r = 0^\circ$ and 90° , (ii) $\Theta_r = 90^\circ$, $\Phi_r = 15^\circ$ and 75° and (iii) $\Theta_r = 60^\circ$, $\Phi_r = 15^\circ, 30^\circ, 45^\circ$ and 60° . The maximum magnitude of $\mu_0 \mathbf{H}$ is 25 T and the results for every 2 T are marked. Corresponding to the three cases of field directions different rotational behaviour of \mathbf{J}_s is obtained:

(i) for field directions in the planes c_r - c_t ($\Phi_r = 0^\circ$) or c_r - b_m ($\Phi_r = 90^\circ$) the grain polarization rotates like in a uniaxial material, especially for \mathbf{H} parallel to c_t or b_m ($\Theta_r =$

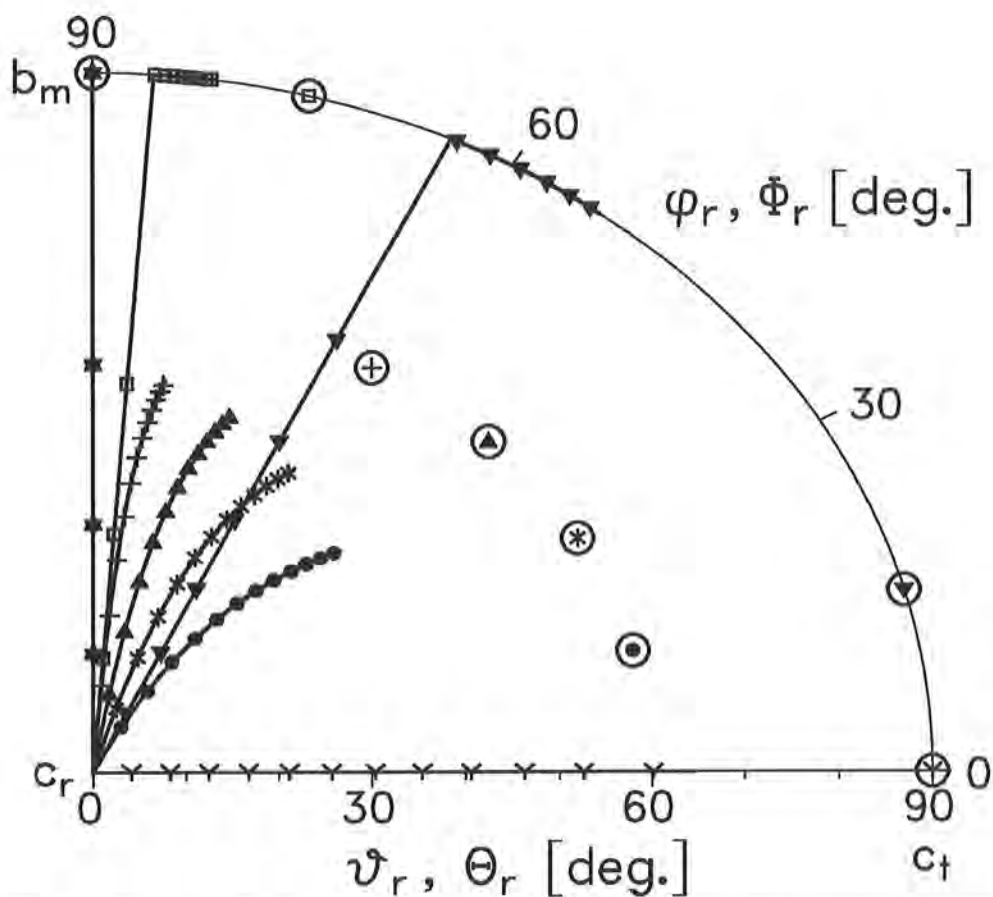


Fig.2: Polar presentation of polarization rotation due to increasing fields acting on a material of monoclinic structure with the special type of magnetic anisotropy as that of $\text{Sm}_3(\text{Fe,M})_{29}\text{N}_4$ where c_r is the EMD and c_t is the magnetically hard direction. The polar angles of magnetization and field, ψ_r and Θ_r , are related to the EMD pointing out of the page. The corresponding azimuth angles, φ_r and Φ_r , vary from 0 (c_t axis) to 90 deg. (b_m axis). The solutions for every 2 T of field magnitude are presented by special symbols. The field directions are indicated by corresponding circled symbols. Note that the polarization direction may strongly deviate from the plane given by the EMD and the field.

90°) the polarization component in field direction increases linearly with increasing \mathbf{H} and is aligned parallel to \mathbf{H} for $\mu_0 H \geq (2K_{1\vartheta} + 4K_{1\varphi}) / J_s$ (for $\Phi_r = 0^\circ$) or $\mu_0 H \geq 2K_{1\vartheta} / J_s$ ($\Phi_r = 90^\circ$). Note, that the factor 4 in front of $K_{1\varphi}$ should not be confused with that of K_2 for uniaxial materials but is caused by the definition in Eq.3.

(ii) for \mathbf{H} in a plane perpendicular to the EMD ($\Theta_r = 90^\circ$) but arbitrary direction inside this plane ($0^\circ < \Phi_r < 90^\circ$) the polarization rotates first in a plane with constant φ_r . Depending on Φ_r the polarization is oriented perpendicularly to the EMD (c_r) for field

values in between the limits given for case (i). For higher fields the polarization rotates further in the plane perpendicular to the EMD ($\vartheta_r = 90^\circ$, φ_r increasing with H). It should be noted that this change in the rotation direction of the polarization can be detected by measurement of the second derivative d^2J/dH^2 (SPD method¹²).

iii) For arbitrary field direction ($0^\circ < \Theta_r < 90^\circ$, $0^\circ < \Phi_r < 90^\circ$) \mathbf{J}_s rotates out of the EMD on curves which can be considerably bent toward the c_r - c_t -plane in which the strongest anisotropy is found. For the examples shown in Fig.2 the initial rotation of \mathbf{J}_s takes place with an azimuth angle φ_r much larger than the azimuth Φ_r of the field \mathbf{H} .

4.2. Fit of demagnetization curves for materials of monoclinic structure

For the calculation of the polarization J of polycrystalline samples which is usually measured in field direction the contributions of the differently oriented grains have to be summed up. Therefore, for each grain orientation the equilibrium orientation of \mathbf{J}_s has to be determined as described in the previous subsection and the resulting component of \mathbf{J}_s in field direction has to be weighted by the orientation density of the grain orientation under consideration, i.e. the texture. However, as shown in Fig.2, not only the orientation of the grains EMD but also the orientation of the magnetically hard direction has to be known. The latter requires considerations beyond the scope of uniaxial materials where, in lowest order in the direction cosines, only the c -axis orientation is of interest for magnetism. Due to the sample preparation process the EMD's of the grains are aligned by the applied magnetic field. Hence, we expect a distribution of the EMD of the grains inside the sample to be of Gaussian type as in the case of uniaxial materials¹²

$$f(\psi) \propto \exp(-\psi^2 / 2\sigma_g^2) \quad (7)$$

where ψ is the angle between the local EMD and the texture axis (defined by the aligning field) and σ_g is the texture parameter. The magnetically hard direction of the grains is assumed to be randomly distributed. It should be noted that this magnetic texture corresponds to different crystallographic textures depending on the orientation of the EMD and the magnetically hard direction with respect to the crystallographic axes. Starting from a set of parameters $K_{1\vartheta}$, $K_{1\varphi}$, σ_g , J_w demagnetization curves in the first quadrant of the J - H -plane can be calculated. Here, J_w denotes the contribution of a soft magnetic phase (e.g. α -Fe) to the sample polarization which can be compared with the portion of this phase determined by other techniques (e.g. X-ray diffraction). The named parameters are determined by a least mean square fit adjusting the calculated demagnetization curves to polarization values measured for fields applied parallel and perpendicularly to the sample texture axis. The result of the fit procedure for the $\text{Sm}_3(\text{Fe,Ti})_{29}\text{N}_4$ -sample is shown in Fig.3 by lines whereas the measured polarizations are presented by markers (only every second data point is shown). The residual standard

deviation 0.55 (mT)^2 is typical for our fit results and compares to the accuracy of the polarization measurement (about 3 mT). Internal stray fields were taken into account by

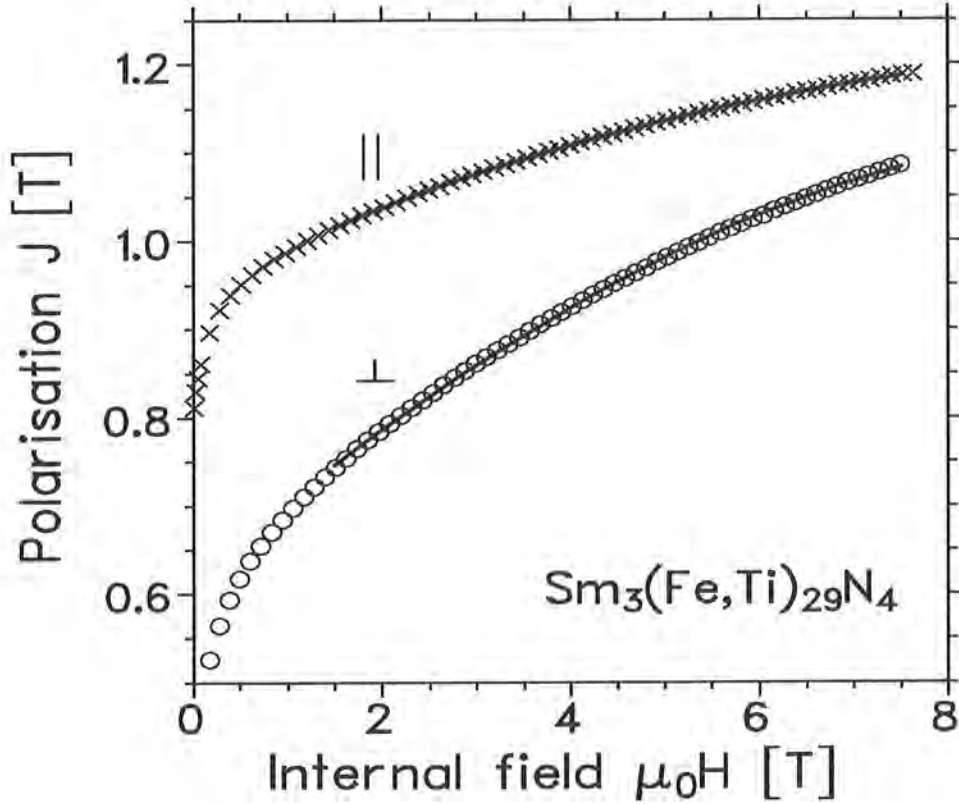


Fig.3: Comparison between calculated (lines) demagnetization curves and polarization values measured parallel (x) and perpendicular (O) to the texture axis of a $\text{Sm}_3(\text{Fe,Ti})_{29}\text{N}_4$ -sample. The fit procedure reveals the anisotropy constants $K_{1\vartheta} = 2.9 \text{ MJm}^{-3}$ and $K_{1\varphi} = 2.4 \text{ MJm}^{-3}$.

the sample demagnetization factor only and therefore polarization values measured at fields $\mu_0 H \leq 1.6 \text{ T}$ where interactions influence the measured sample polarization consider-

Tab.1: Results for the anisotropy constants $K_{1\vartheta}$, $K_{1\varphi}$, the saturation polarization J_s and the texture parameter σ_g of samples prepared from the parent compounds $\text{R}_3(\text{Fe,Ti})_{29}$ obtained by fitting of demagnetization curves.

sample	$K_{1\vartheta}$ [MJm ⁻³]	$K_{1\varphi}$ [MJm ⁻³]	J_s [T]	σ_g [deg.]
$\text{Sm}_3(\text{Fe,Ti})_{29}$	1.4	0.4	1.13	35
$\text{Nd}_3(\text{Fe,Ti})_{29}$	0.3	0.3	1.32	48
$\text{Pr}_3(\text{Fe,Ti})_{29}$	0.5	1.3	1.21	102
$\text{Ce}_3(\text{Fe,Ti})_{29}$	0.6	2.3	0.95	116

Tab.2: Fit results for the anisotropy constants $K_{1\vartheta}$, $K_{1\varphi}$, the saturation polarization J_s and the texture parameter σ_g of the investigated $R_3(\text{Fe,Ti})_{29}\text{N}_4$ samples (*value taken from Ref. 1)

sample	$K_{1\vartheta}$ [MJm ⁻³]	$K_{1\varphi}$ [MJm ⁻³]	J_s [T]	σ_g [deg.]
$\text{Sm}_3(\text{Fe,Ti})_{29}\text{N}_4$	2.9	2.4	1.30	39
$\text{Nd}_3(\text{Fe,Ti})_{29}\text{N}_4$	2.2	2.3	1.54	49
$\text{Pr}_3(\text{Fe,Ti})_{29}\text{N}_4$	1.7	3.2	1.56*	57

ably were neglected in the fit procedure. The results for the different investigated samples prepared from the parent and the nitrided compounds are summarized in Tab.1 and Tab.2, respectively. The results for J_s are in agreement with those given in Ref. 1. It should be noted that the crystallographic orientation of the EMD cannot be derived from the results of the fit procedure alone. However, for the nitrided compounds where the magnetic anisotropy is dominated by the influence of the N atoms the direction of the EMD can be derived from the superposition principle as introduced in section 3.2. Due to the different signs of the Stevens coefficients of the R's the determined anisotropy constants $K_{1\vartheta}$ and $K_{1\varphi}$ are related to different crystallographic axes. In case of $R = \text{Sm}$ the EMD is the c_r axis whereas the c_t axis is the hard direction. Therefore one obtains $K_{1\vartheta} = (2v_r/3v_m)K_{1,r}$ and $K_{1\varphi} = -(v_t/2v_m)K_{1,t}$ whence $K_{1,r} = 4.4 \text{ MJm}^{-3}$ and $K_{1,t} = -12.0 \text{ MJm}^{-3}$. For the Nd and Pr compounds, the c_t axis is the EMD and the c_r axis is the magnetically hard direction: $K_{1\vartheta} = (v_t/v_m)K_{1,t}$ and $K_{1\varphi} = -(v_r/3v_m)K_{1,r}$. This results in $K_{1,r} = -6.9 \text{ MJm}^{-3}$ and $K_{1,t} = 5.5 \text{ MJm}^{-3}$ for $\text{Nd}_3(\text{Fe,Ti})_{29}\text{N}_4$ and $K_{1,r} = -9.6 \text{ MJm}^{-3}$ and $K_{1,t} = 4.3 \text{ MJm}^{-3}$ for $\text{Pr}_3(\text{Fe,Ti})_{29}\text{N}_4$. The volume ratios of the different segments are estimated to $v_r/v_m = 1$ and $v_t/v_m = 0.4$.^{1,9,13} Note that the $K_{1,r}$ obtained for the compounds $R_3(\text{Fe,M})_{29}\text{N}_4$ with $R = \text{Sm}$, Nd agree, as expected, in sign and order of magnitude with the K_1 determined for the $\text{Sm}_2\text{Fe}_{17}\text{N}_3$ and $\text{Nd}_2\text{Fe}_{17}\text{N}_{2.7}$, respectively.^{8,14}

5. Conclusions

In monoclinic materials, even in lowest order of an expansion series in the direction cosines, two anisotropy constants have been needed to describe the magnetocrystalline anisotropy and there is always an easy magnetization direction (EMD). The two-fold monoclinic axis b_m is one of the three principal axes of the magnetocrystalline energy (in lowest order) but is not necessarily the EMD. In our fit procedure for polycrystalline materials the anisotropy constants $K_{1\vartheta}$ and $K_{1\varphi}$ are related to the polar angle ϑ referred to the EMD and the azimuth angle φ referred to the hard magnetization direction (HMD). Therefore, both $K_{1\vartheta}$ and $K_{1\varphi}$ are non-negative by definition. In the case of the

interstitially modified compound $R_3(\text{Fe,Ti})_{29}\text{N}_4$ (with $R = \text{Sm, Nd, Pr}$) the anisotropy energy density f_{Am} has been described by a superposition principle relating f_{Am} to contributions of the 2:17 and 1:12 segments forming the 3:29 structure. By using this model the EMD and HMD could be related to the crystallographic axes. The order of magnitude of the fitted values of $K_{1\delta}$ and $K_{1\phi}$ of $R_3(\text{Fe,Ti})_{29}\text{N}_4$ agree well with those expected from the superposition model. However, the first anisotropy constants for the $\text{Sm}_2\text{Fe}_{17}\text{N}_3$ segment calculated from the fitted results is about a factor two too small compared to the data known for $\text{Sm}_2\text{Fe}_{17}\text{N}_3$ from literature. On the other hand it is well known that in the case of $\text{Sm}_2\text{Fe}_{17}\text{N}_3$ the second anisotropy constant cannot be neglected. Therefore, higher-order contributions of f_{Am} of $R_3(\text{Fe,Ti})_{29}\text{N}_4$ should be taken into account. Furthermore, in a more detailed investigation the anisotropy of the 3d-electron system of the iron has also to be considered.

References

1. J.M.D. Cadogan, H.-S. Li, A. Margarian, J.B. Dunlop, D.H. Ryan, S.J. Collocott and R.L. Davis, *J. Appl. Phys.* **76** (1994) 6138.
2. C.D. Fuerst, F.E. Pinkerton, J.F. Herbst, *J. Magn. Magn. Mater.* **129** (1994) L115.
3. H.-S. Li, J.M. Cadogan, R.L. Davis, A. Margarian and J.B. Dunlop, *Sol. State Commun.* **90** (1994) 487.
4. O. Kalogirou, V. Psycharis, L. Saettas and D. Niarchos, *J. Magn. Magn. Mater.* **146** (1995) 335.
5. F.-M. Yang, B. Nasunjilegal, W. Gong and G. C. Hadjipanayis, *IEEE Trans. MAG-30* (1994) 4957.
6. H.-S. Li and J.M.D. Coey, in Handbook of Magnetic Materials, vol.6, edited by K.H.J. Buschow, North-Holland, Amsterdam 1991, pp 1.
7. J.J.M. Franse and R.J. Radwanski, in Handbook of Magnetic Materials, vol.7, edited by K.H.J. Buschow, North-Holland, Amsterdam 1993, pp 307.
8. K.-H. Müller, D. Eckert, P.A.P. Wendhausen, A. Handstein, S. Wirth, M. Wolf, *IEEE Trans. MAG-30* (1994) 586.
9. D.P.F. Hurley, M. Kuz'min, Qi-nian Qi, and J.M.D. Coey, Proc. 6th Int. Conf. on Ferrites (ICF6), Tokyo 1992, 1096.
10. Ying-chang Yang, Xiao-dong Zhang, Sen-lin Ge, Qi Pan, Lin-shu Kong, Hailin Li, Ji-lian Yang, Bai-sheng Zhang, Yong-fan Ding, Chun-tang Ye, *J. Appl. Phys.* **70** (1991) 6001.
11. Hong Sun, J.M.D. Coey, Y. Otani and D.P.F. Hurley, *J. Phys.: Condens. Matter* **2** (1990) 6465.
12. G. Asti, R. Cabassi, F. Bolzoni, S. Wirth, D. Eckert, P.A.P. Wendhausen and K.-H. Müller, *J. Appl. Phys.* **76** (1994) 6268.
13. Z. Altounion, X. Chen, L.X. Liao, D.H. Ryan and J.O. Ström-Olsen, *J. Appl. Phys.* **73** (1993) 6017.
14. M. Katter, J. Wecker, C. Kuhrt, L. Schultz, X.C. Kou and R. Grössinger, *J. Magn. Magn. Mater.* **111** (1992) 293.